

Supporting Information (S-1)

Sensitive Detection of Black Powder by Stand-Alone Ion Mobility Spectrometer Embedded a Titration Region

Xixi Liang,^{†,‡} Qinghua Zhou,^{†,‡} Weiguo Wang,[†] Xin Wang,[†] Wendong Chen,[†]

Chuang Chen,^{†,‡} Yang Li,[†] Keyong Hou,[†] Jinghua Li,[†] Haiyang Li^{,†}*

[†]Dalian Institute of Chemical Physics, Chinese Academy of Sciences, Dalian, 116023,

People's Republic of China

[‡]Graduate University of Chinese Academy of Sciences, Beijing, 100039, People's

Republic of China

*E-mail: hli@dicp.ac.cn. Fax: +86-411-84379517.

ABSTRACT

This supporting information provides additional information on the following aspects:

To investigate the efficient reactant ions for ionizing sulfur, the modified ion mobility spectrometer (Figure S-1) with lateral sample introduction through the side of the drift tube in two different carrier gas modes (CH_2Cl_2 doped and purified air) were employed; In the conventional IMS, the effect of different concentration of dichloromethane on the detection of sulfur, was also investigated, as shown in Figure S-2; The negative mass spectrum in ^{63}Ni source for detection 1 ng sulfur via homemade ion trap mass spectrometer was shown in Figure S-3; The negative mass spectra in ^{63}Ni source for detection of black powder and other common explosives were depicted in Figure S-4; In the final section, the IMS parameters in this work were summarized in Table S-1.

Chemicals. Sulfur is considered as the substitute of black powder. Pure sulfur and dichloromethane was purchased from Tianjin Kermel Chemical Reagent Co., Ltd. Black powders, firecracker, trinitrotoluene (TNT), ammonium nitrate fuel oil (ANFO), and pentaerythritol tetranitrate (PETN) were all commercial grade. Sulfur and explosives solutions with different concentrations were prepared by successive dilution of their stock solutions (50 ng/ μL) in acetone.

2, To investigate the efficient reactant ions for ionizing sulfur, two separate modes of carrier gas involving chlorinated hydrocarbons doped air and purified air were

periodically switched into the ionization region to produce different reactant ions, while the sample vapor was introduced into the titration region through the side of the drift tube, as illustrated in Figure S-1. Therefore, if the product ions of the samples could be created by these two different reactant ions would be clearly investigated in the titration region, separately.

Figure 2a shows the typical IMS spectra for detecting the 100 pg sulfur in these two modes. In one mode of using pure air as carrier gas, the product ions peak (PIP) of sulfur was obtained but with serious overlapping with $\text{O}_2^-(\text{H}_2\text{O})_n$ reactant ions peak (RIP). The R_s between RIP centered at 6.86 ms and the PIP centered at 7.08 ms is just 0.43. In the other mode, when chlorinated hydrocarbons mixed air are present in the ionization reaction region, no obvious product ions of black powder but only the predominant $\text{Cl}^-(\text{H}_2\text{O})_n$ reactant ions appeared at 5.52 ms are observed in the Figure 2a (red line). It is indicated that the $\text{O}_2^-(\text{H}_2\text{O})_n$ reactant ions were directly responsible for the formation of product ions for black powder, while the $\text{Cl}^-(\text{H}_2\text{O})_n$ reactant ions hindered the formation of ionic sulfur allotropes. This conclusion was further confirmed from Figure 2b, which illustrates the time profile of PIP intensity for continuously measuring sulfur with initial amounts of 50 ng by periodically switching of with/ without CH_2Cl_2 doped carrier gas modes with 20 seconds per cycle time. In this experiment, once the carrier gas is switched from the CH_2Cl_2 doped air to the purified air, the product ions intensity for BP present at 7.08 ms is sharply increased from 20 mv to 350 mv. The good repeatability

obtained in at least five periods clearly proves that the $O_2^-(H_2O)_n$ reactant ions can ionize the black powder, unfortunately, the $Cl^-(H_2O)_n$ reactant ions are found to suppress the ionization of sulfur.

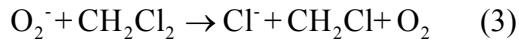
2, Figure S-2 showed the ion mobility spectra of different concentration of dichloromethane added in the carrier gas through the ionization region (a) without sulfur, (b) with 100 pg sulfur with a conventional ion mobility spectrometry similar to the previous literature.¹ When the concentration of dichloromethane was below 2.5 ppm, the signal of $O_2^-(H_2O)_n$ is strong, and the peaks for sulfur were overlapped with that of $O_2^-(H_2O)_n$. Increasing the concentration of dichloromethane, the signal of $O_2^-(H_2O)_n$ is decreased rapidly as shown in Figure S-2a; and the signal of sulfur also is decreased simultaneously as shown in Figure S-2b and disappeared when the concentration of dichloromethane is higher than 16 ppm. Thus, it can be seen that lower concentration of dichloromethane cannot result to the similar results as shown with the titration region, indicating that the conventional dopant method was not successful in resolving peak overlap of BP and RIP.

3, The actual ionization process is not known clearly and may be very complex. In this case, we only discussed the reactivity of charge-transfer reactions between O_2^- (or S_3^-) with dichloromethane based on the Gibbs energy of the reactions ($\Delta_r G$).

The thermodynamic data used are: $EA(S_3) = 2.310\text{ eV}$ (222.88 KJ/mol),² $EA(Cl) = 3.613\text{ eV}$ (348.60 KJ/mol),² $EA(O_2) = 0.448\text{ eV}$ (43.22 KJ/mol),² and the bond

dissociation energy (BDE = 325.9 KJ/mol) of Cl-CH₂Cl.³ Since there is no available standard molar entropy⁴ for some ions and radicals, such as O₂⁻, Cl⁻, S₃⁻, S₄⁻, CH₂Cl, we need to estimate from similar atoms or molecules. Firstly, the standard molar entropy of atom/molecule are similar to their corresponding ions, *i.e.*, $S(\text{O}_2) \approx S(\text{O}_2^-)$, $S(\text{Cl}) \approx S(\text{Cl}^-)$, $S(\text{S}_3) \approx S(\text{S}_3^-)$, $S(\text{S}_4) \approx S(\text{S}_4^-)$. Secondly, the entropy difference: $S(\text{CH}_2\text{Cl}_2) - S(\text{CH}_2\text{Cl}) \approx S(\text{CH}_3\text{Cl}) - S(\text{CH}_3) = 234.6 - 194.2 \approx 40 \text{ J/mol K}$.

For reaction (3):



$$\begin{aligned} \Delta_r H(3) &\approx \text{BDE}(\text{Cl}-\text{CH}_2\text{Cl}) - \text{EA}(\text{Cl}) + \text{EA}(\text{O}_2) \\ &= 325.9 - 348.6 + 43.22 \\ &= 20.52 \text{ KJ/mol} \end{aligned}$$

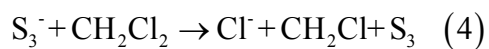
$$\begin{aligned} \Delta_r S(3) &= S(\text{Cl}^-) + S(\text{CH}_2\text{Cl}) + S(\text{O}_2) - S(\text{CH}_2\text{Cl}_2) - S(\text{O}_2^-) \\ &= S(\text{Cl}^-) + (S(\text{CH}_2\text{Cl}) - S(\text{CH}_2\text{Cl}_2)) + (S(\text{O}_2) - S(\text{O}_2^-)) \\ &\approx 165.19 - 40 \\ &= 125.19 \text{ J/mol} \cdot \text{K} \end{aligned}$$

Under the experimental temperature of 363 K, Gibbs energy of reaction (3)

$$\begin{aligned} \Delta_r G(3) &= \Delta_r H(3) - T\Delta_r S(3) \\ &= 20.52 - 363 \times 125.19 \times 10^{-3} \\ &= -24.92 \text{ KJ/mol} \end{aligned}$$

Although the standard enthalpy of reaction is an endothermic reaction, the negative Gibbs energy of reaction indicated that the reaction (3) is allowed in thermodynamics.

Similarly, for reaction (4):



$$\begin{aligned}\Delta_r H(4) &\approx \text{BDE}(\text{Cl}-\text{CH}_2\text{Cl}) - \text{EA}(\text{Cl}) + \text{EA}(\text{S}_3) \\ &= 325.9 - 348.6 + 222.88 \\ &= 200.18 \text{ KJ/mol}\end{aligned}$$

$$\begin{aligned}\Delta_r S(4) &= S(\text{Cl}^-) + S(\text{CH}_2\text{Cl}) + S(\text{S}_3) - S(\text{CH}_2\text{Cl}_2) - S(\text{S}_3^-) \\ &= S(\text{Cl}^-) + (S(\text{CH}_2\text{Cl}) - S(\text{CH}_2\text{Cl}_2)) + (S(\text{S}_3) - S(\text{S}_3^-)) \\ &\approx 165.19 - 40 \\ &= 125.19 \text{ J / mol} \cdot \text{K}\end{aligned}$$

$$\begin{aligned}\Delta_r G(4) &= \Delta_r H(4) - T\Delta_r S(4) \\ &= 200.18 - 363 \times 125.19 \times 10^{-3} \\ &= 154.73 \text{ KJ/mol}\end{aligned}$$

The positive Gibbs energy of reaction indicated that the reaction (4) is prohibited in thermodynamics.

REFERENCES

- (1) Zhou, Q.; Wang, W.; Cang, H.; Du, Y.; Han, F.; Chen, C.; Cheng, S.; Li, J.; Li, H. *Talanta* **2012**, 98, 241-6.
- (2) <http://webbook.nist.gov/chemistry/>.
- (3) Luo, Y. R. *Comprehensive Handbook of Chemical Bond Energies*; CRC Press: Boca Raton, FL, 2007.
- (4) Lide, D. R. *CRC Handbook of Chemistry and Physics, Standard Thermodynamic properties of chemical substances*; CRC Press: Boca Raton, FL, 2004.

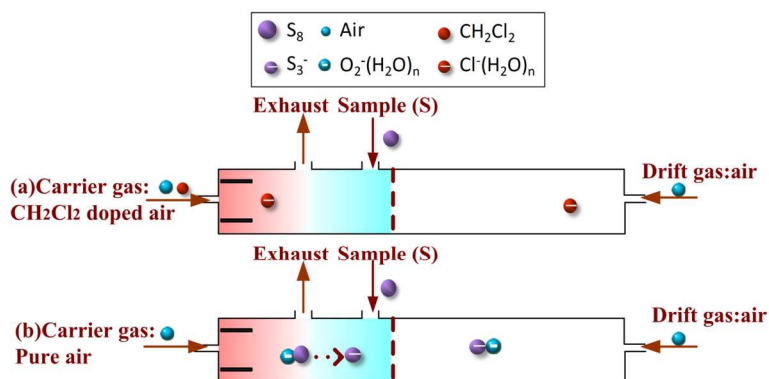


Figure S-1. Schematic drawing of the ion mobility spectrometer with lateral sample introduction through the side of the drift tube in two different carrier gas modes: (a) CH_2Cl_2 doped and (b) purified air.

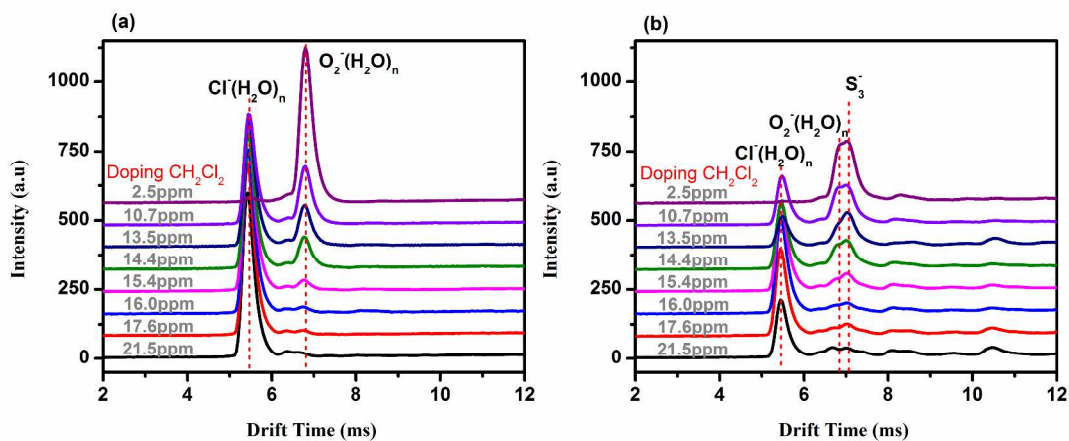


Figure S-2. Ion mobility spectra for different concentration of dichloromethane adding into carrier gas in conventional IMS (a) without sulfur, (b) with 100 pg sulfur.

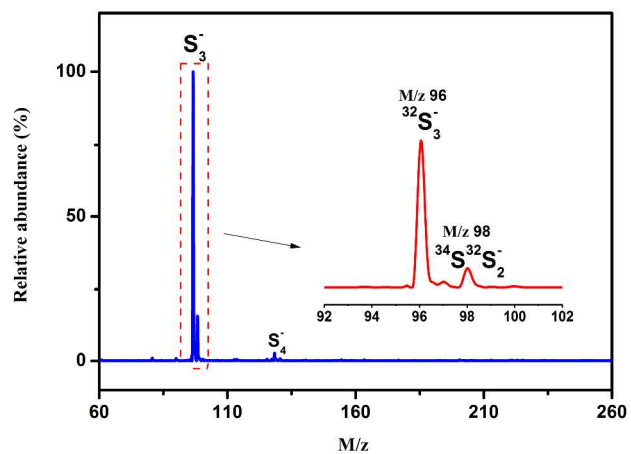


Figure S-3. The negative ion trap mass spectrum in ^{63}Ni source for detecting 1 ng sulfur with CH_2Cl_2 as titration reagent.

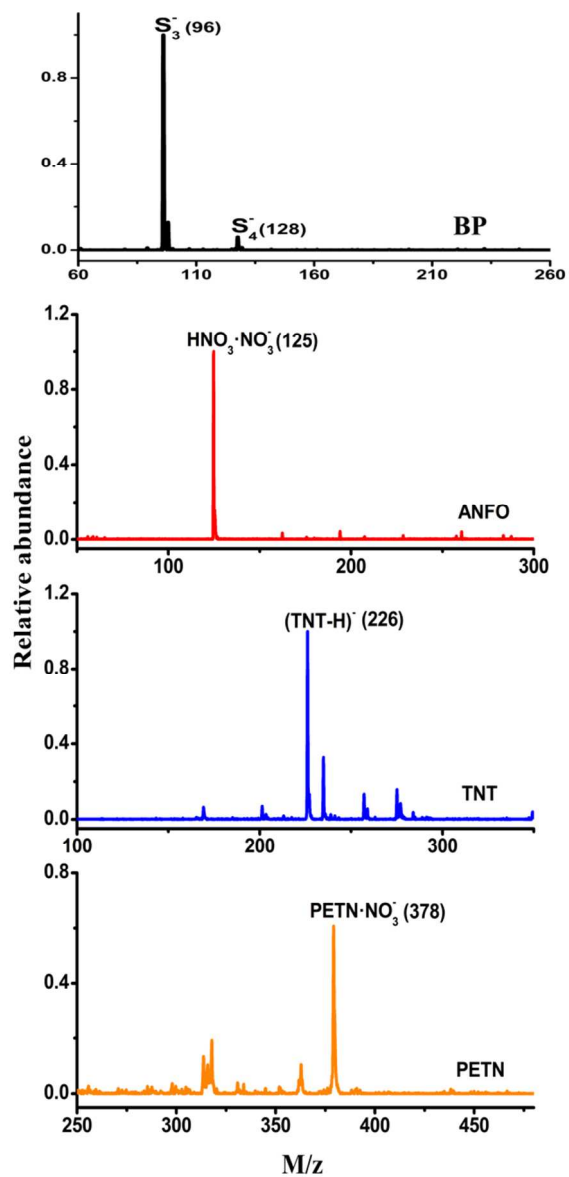


Figure S-4. The negative mass spectra in ^{63}Ni source for detecting of BP, ANFO, TNT, and PETN with CH_2Cl_2 as titration reagent.

Table S-1. The TR- IMS parameters used in this work

Ionization source	^{63}Ni in negative mode
Desorption temperature	180°C
Drift tube temperature	90°C
Voltage drop	5000 V
Ionization region length	24 mm
Titration region length	16 mm
Drift region length	90 mm
Carrier gas	Purified Air
Drift gas	Purified Air
Titration gas	Purified Air
Titration Reagent	CH_2Cl_2
Reagent concentration	20 ppm
Reagent gas flow rate	200 mL min ⁻¹
Carrier gas flow rate	200 mL min ⁻¹
Drift gas flow rate	600 mL min ⁻¹